

**Critical adsorption at chemically structured substrates**

Monika Sprenger, Frank Schlesener, and S. Dietrich

*Max-Planck-Institut für Metallforschung, Heisenbergstrasse 3, D-70569 Stuttgart, Germany**and Institut für Theoretische und Angewandte Physik, Universität Stuttgart,**Pfaffenwaldring 57, D-70569 Stuttgart, Germany*

(Received 24 January 2005; published 27 May 2005)

We consider binary liquid mixtures near their critical consolute points and exposed to geometrically flat but chemically structured substrates. The chemical contrast between the various substrate structures amounts to opposite local preferences for the two species of the binary liquid mixtures. Order parameter profiles are calculated for a chemical step, for a single chemical stripe, and for a periodic stripe pattern. The order parameter distributions exhibit frustration across the chemical steps which heals upon approaching the bulk. The corresponding spatial variation of the order parameter and its dependence on temperature are governed by universal scaling functions which we calculate within mean field theory. These scaling functions also determine the universal behavior of the excess adsorption relative to suitably chosen reference systems.

DOI: 10.1103/PhysRevE.71.056125

PACS number(s): 64.60.Fr, 68.35.Rh, 61.20.-p, 68.35.Bs

**I. INTRODUCTION**

Chemically structured substrates have gained significant importance within the last few years. Since it is possible to produce networks of chemical lanes at the micrometer scale and even below, these chemically structured substrates have applications in microreactors, for the “laboratory on a chip,” and in chemical sensors [1,2]. They can operate with small amounts of reactants, which is important when investigating expensive substances and substances that are available only in small amounts, like biological material, or when dealing with toxic or explosive materials. At these small scales the interaction of the fluids with the substrate becomes important and there is the challenge of controlling the distribution and the flow of the fluids on these structures.

In the following we investigate three different types of chemically structured substrates, as shown in Fig. 1. First we analyze fluid structures at a chemical step [see Fig. 1(a)] which is important for understanding the local properties of fluids at the border of stripes. Next we consider a single chemical stripe [see Fig. 1(b)] as the simplest chemical surface pattern, and finally we study a periodic stripe pattern [see Fig. 1(c)] as the paradigmatic case for the investigation of adsorption at heterogeneous surfaces.

The chemical contrast on the substrates acts on the adjacent liquid [3,4]. In order to impress the chemical pattern of the substrate on a one-component liquid, the chemical structure has to be chosen as a pattern of lyophobic and lyophilic regions. For binary liquid mixtures one chooses a pattern of two different substrate types, such that one component is preferred by one substrate type and the second component by the other substrate type. This lateral structuring of the substrate causes a rich fluid-substrate interface structure which typically depends on the molecular details of the local force fields. However, in this study we focus on the particular case of the fluid being close to a second-order phase transition. This is either the liquid-vapor critical point of a one-component liquid or the critical demixing transition of a binary liquid mixture. In these cases the ensuing critical phenomena are to a large extent universal in character, i.e., they

render molecular details irrelevant in favor of universal scaling functions by involving spatial variations on the scale of the diverging correlation length. Near the critical point the surface patterning acts like a laterally varying surface field of alternating sign. This generates an order parameter profile characterizing critical adsorption of opposite sign such that the system is frustrated across the chemical steps. Upon approaching the bulk of the fluid this frustration is healed and the healing is expected to be governed by universal scaling functions. In addition, the substrate patterning results in a change of the excess amount of adsorbed fluid with respect to the case of critical adsorption on a homogeneous substrate. The excess adsorption is expected to be governed by universal scaling functions, too.

It is the purpose of this contribution to describe this scaling in terms of general renormalization group arguments and to calculate the corresponding universal scaling functions to lowest order, i.e., within mean field theory. If, as is actually the case, the size of the lateral structures is comparable with the range of the correlation length, which can reach up to 100 nm close to the critical point, one can expect a rich interplay between the externally imprinted patterns and the critical phenomena characterized by the correlation length.

**A. Critical phenomena**

In order to describe critical phenomena [5,6] one distinguishes properties to classify them. Starting with unconfined systems one introduces the so-called bulk universality classes which are characterized by critical exponents and amplitudes that describe the dependence of various quantities, e.g., the order parameter and the correlation length, on the reduced temperature  $t=(T-T_c)/T_c$  upon approaching the critical temperature  $T_c$ . These critical exponents are universal, i.e., the same for all members of a universality class. The amplitudes usually are nonuniversal, whereas the number of independent nonuniversal amplitudes is limited; any nonuniversal amplitude can be expressed in terms of these independent nonuniversal amplitudes and universal amplitude ratios.

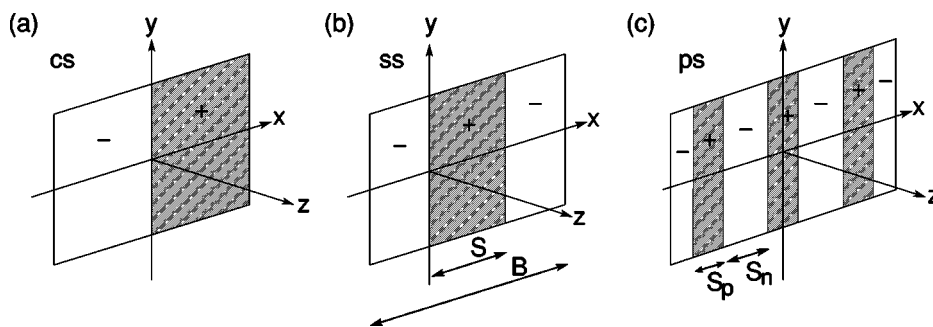


FIG. 1. The different chemical substrate structures studied in this article: (a) chemical step (CS), (b) single stripe (SS), (c) periodic stripes (PS). All systems are translationally invariant in the  $y$  direction. The shading indicates different local preferences for, e.g., the two components of a binary liquid mixture exposed to the geometrically flat surface of macroscopically large lateral extension  $B$ .

One-component fluids near their liquid-vapor critical point and binary liquids near their demixing critical point belong to the Ising universality class, for instance uniaxial ferromagnets. These systems have two independent nonuniversal amplitudes. In this sense our subsequent analysis holds for all systems encompassed by the Ising universality class.

The order parameter  $\phi$  indicates the degree of order in the system and has to vanish above the critical temperature while below the critical temperature it takes a finite value. It is described by the universal critical exponent  $\beta$  and a nonuniversal amplitude  $a$ :  $\phi(t) = a|t|^\beta$ . For a one-component fluid  $\phi$  is the difference between the density and its value at the critical point. In the case of a binary liquid mixture it is chosen as the difference between the concentration of one fluid component and its concentration at the critical demixing point.

The correlation length is defined by the exponential decay of the bulk two-point correlation function  $G(r)$  for large distances ( $r \rightarrow \infty$ ) at temperatures off criticality ( $T \neq T_c$ ) and it is denoted as  $\xi^+$  above and as  $\xi^-$  below the critical temperature. It diverges according to the power law  $\xi^\pm = \xi_0^\pm |t|^{-\nu}$  with the universal critical exponent  $\nu$  and the nonuniversal amplitudes  $\xi_0^\pm$ . Their ratio  $\xi_0^+/\xi_0^-$  is, however, universal. If the critical medium is brought near a substrate, surface universality classes come into play, which we shall discuss in Sec. II.

## B. Experimental methods

Different techniques to produce chemical structures in the range of micro- and nanometers have been established [7]. In order to obtain topologically flat but chemically structured substrates one can take advantage of the self-ordering mechanism of self-assembled monolayers (SAMs) in using block copolymers or mixtures of polymers which form structures while demixing [3,8,9]. The morphology and domain size of these structures depend on different characteristics of the materials and of the formation process. Another possibility to produce structured substrates is to change the functionality of the SAMs partially by irradiating a homogeneous SAM that is covered with a mask that carries the desired structure [10]. A third method is the so-called microcontact printing [11] where samples, e.g., produced with lithography, are used as a mold for an elastomer stamp. The structure of the original is copied by stamping a “thiol ink” on gold

covered substrates which chemisorbs there and forms a SAM. The empty spaces between the patterns of the stamped structure can be filled with a second thiol with a different functional end group such that a topologically flat but chemically structured substrate is built up. As a last method we mention the exposure of oxidated titanium surfaces to uv light [12–14].

In order to investigate the structural properties of fluid systems near surfaces, various experimental methods have been developed: Ellipsometry and especially phase modulated ellipsometry were established in Refs. [15,16] more than 20 years ago and are still powerful tools [17,18]. An incident light beam is reflected by the surface of interest and the ratio of the complex reflection amplitudes for polarizations parallel and perpendicular to the plane of incidence (“coefficient of ellipsometry” or “ellipticity”) is measured. The order parameter is modeled and related to the ellipticity via the spatially varying dielectric constant and can then be compared with the measured value. In neutron or x-ray reflectometry one measures the reflectivity as a function of the momentum transfer normal to the surface of the sample. This reflectivity spectrum is related to the refractive index profile, which itself is associated with the profile of the order parameter [18–22]. A more direct measurement of the adsorption of a component to a substrate can be carried out with a differential refractometer [23,24]. Here a laser beam passes a measurement cell consisting of two compartments filled with the fluid of interest and a reference liquid, respectively. The intensity of the deflected beam is proportional to their difference in refractive index. By comparing this measured intensity with the one of a beam deflected by a measurement cell filled with a liquid with known interfacial properties and the reference liquid, one is able to infer the properties of the fluid of interest.

With these methods critical adsorption on homogeneous substrates has been experimentally investigated (see Refs. [25,26] and references therein). On chemically structured substrates mostly wetting experiments have been performed [27–29]. The present paper extends theoretical work on critical adsorption on chemically homogeneous [30–33] and topologically [34] structured surfaces and work on wetting phenomena at chemically structured substrates [35–39] to the case of critical adsorption on geometrically flat, but chemically structured surfaces.

The remainder of this paper is organized as follows. In Sec. II we introduce our model and in order to set the stage we recall previous results on critical adsorption at homogeneous substrates. In Sec. III we present our results for the critical adsorption at chemically structured substrates. We summarize our findings in Sec. IV.

## II. CRITICAL ADSORPTION AT HOMOGENEOUS SUBSTRATES

Boundaries, which come into play when investigating confined systems, induce deviations from the bulk behavior. Near a critical point the Ising bulk universality class splits into three possible surface universality classes (denoted as normal, special, and ordinary surface universality classes, respectively) characterized by surface critical exponents and amplitudes [30,31]. The boundary conditions applied to the system determine the surface universality class, to which the system belongs. The behavior of the bulk is not affected by the boundaries.

It has turned out that in the sense of renormalization group theory it is sufficient to describe the presence of the substrate by a surface field  $h_1$  and the so-called surface enhancement  $c$  [31]. [These names originate from the corresponding description of surface magnetic phenomena [30,31]; see also Eq. (7).] The surface enhancement is related to the couplings between the ordering degrees of freedom at the surface.

The so-called ordinary surface universality class is characterized by a vanishing surface field and a positive surface enhancement ( $h_1=0, c>0$ ) which suppresses the order parameter at the surface below its bulk value. For magnetic systems this effect of missing bonds is the generic case.

The special surface universality class, describing a multicritical point, requires in addition to a vanishing surface field a surface enhancement which within mean field theory vanishes ( $h_1=0, c=0$ ) and causes a flat order parameter profile in the vicinity of the substrate; fluctuations induce a divergence of the order parameter profile at the surface.

The normal surface universality class is characterized by a nonvanishing surface field and the absence of the surface enhancement ( $|h_1|>0, c=0$ ), which leads to an order parameter value at the surface larger than in the bulk, even above the critical temperature where the bulk value of the order parameter is 0. For fluid systems the normal surface universality class is the generic case. In contrast, in the context of magnetism an order parameter which is larger at the surface than its value in the bulk can be obtained in the absence of surface fields but for a negative surface enhancement ( $h_1=0, c<0$ ). Since this is rather uncommon for magnetic systems, the normal surface universality class is also referred to as the so-called extraordinary surface universality class. The fact that the normal and the extraordinary cases are equivalent and identical at their fixed points, ( $|h_1|\rightarrow\infty, c=0$ ) for fluid systems and ( $h_1=0, c\rightarrow-\infty$ ) for magnetic systems, and thus identical with respect to their asymptotic behavior, was predicted by Bray and Moore [40] and later proven by Burkhardt and Diehl [41]. In the following we

shall focus on the normal and extraordinary surface universality classes, respectively.

A homogeneous substrate confining a binary liquid mixture inevitably has a preference for one of the two components. This preference becomes pronounced at the critical point and leads to an enrichment of the preferred component at the substrate. At the critical temperature the local order parameter profile decays algebraically toward its bulk value. This phenomenon has been called critical adsorption [32].

In the case of planar homogeneous substrates in addition to the correlation length  $\xi^\pm$  the distance  $z$  from the substrate is the other relevant length scale. If this length is scaled with the bulk correlation length  $\xi^\pm$ , the order parameter profile  $\phi(z, t)$  takes the following scaling form at the fixed points ( $|h_1|\rightarrow\infty, c=0$ ) and ( $h_1=0, c\rightarrow-\infty$ ), respectively:

$$\phi(z, t) = a|t|^\beta P^\pm\left(w = \frac{z}{\xi^\pm}\right) \quad \text{for } t \geq 0, \quad (1)$$

with the scaling variable  $w = z/\xi^\pm$ , which describes the distance from the substrate in units of the correlation length  $\xi^\pm$ .

The scaling functions  $P^\pm(w)$  are universal after fixing the nonuniversal amplitude  $a$  and the nonuniversal amplitude  $\xi_0^\pm$  of the correlation length  $\xi$ . (Recall that the ratio  $\xi_0^+/ \xi_0^-$  is universal and therefore the amplitude  $\xi_0^-$  is fixed along with the amplitude  $\xi_0^+$ .) The amplitude  $a$  is chosen in such a way that the scaling function  $P^-(w)$  below the critical temperature tends to 1 for large distances from the substrate, i.e., the amplitude  $a$  corresponds to the amplitude of the bulk order parameter  $\phi(z\rightarrow\infty, t<0) = a|t|^\beta$ . With this choice one finds the following behavior of the scaling functions:

$$P^\pm(w \rightarrow 0) \sim w^{-\beta/\nu}, \quad (2)$$

$$P^+(w \rightarrow \infty) \sim e^{-w}, \quad (3)$$

$$P^-(w \rightarrow \infty) - 1 \sim e^{-w}. \quad (4)$$

Away from the renormalization group fixed point the surface field  $h_1$  and the surface enhancement  $c$  have finite values. They appear as additional parameters in the scaling functions with powers of the reduced temperature as prefactor due to scaling with the correlation length:

$$\phi(z, t) = a|t|^\beta P^\pm(|t|^\nu (\xi_0^\pm)^{-1} z, |t|^{-\Delta_1} (\xi_0^\pm)^{d/2} h_1, |t|^{-\Phi} \xi_0^\pm c), \quad (5)$$

where  $\Delta_1$  and  $\Phi$  are surface critical exponents [31] and  $d$  denotes the spatial dimension of the system.

The explicit calculation of the order parameter profiles  $\phi(z, t)$  starts from the following fixed point Hamiltonian  $\mathcal{H}[\phi] = \mathcal{H}_b[\phi] + \mathcal{H}_s[\phi]$ , which separates into the bulk part  $\mathcal{H}_b[\phi]$  in the volume  $V$  and the surface part  $\mathcal{H}_s[\phi]$  on the surface  $S$  [30,31]:

$$\mathcal{H}_b[\phi] = \int_V d^{d-1} \mathbf{r}_\parallel dz \left( \frac{1}{2} (\nabla \phi)^2 + \frac{1}{2} \tau \phi^2 + \frac{u}{4!} \phi^4 \right), \quad (6)$$

$$\mathcal{H}_s[\phi] = \int_S d^{d-1} \mathbf{r}_{\parallel} \left( \frac{1}{2} c \phi^2 - h_1 \phi \right). \quad (7)$$

Here  $\tau$  is proportional to the reduced temperature  $t$ ,  $u > 0$  stabilizes the Hamiltonian  $\mathcal{H}[\phi]$  for temperatures below the critical point ( $T < T_c$ ), and  $(\nabla \phi)^2$  penalizes spatial variations;  $\mathbf{r}_{\parallel}$  is a vector parallel to the substrate. The order parameter  $\phi$  is fluctuating around a mean value  $\langle \phi \rangle$ . Each configuration  $\phi$  contributes to the partition function  $Z$  with the statistical Boltzmann weight  $e^{-\mathcal{H}[\phi]}$ :

$$Z = \int D\phi (e^{-(\mathcal{H}_b[\phi] + \mathcal{H}_s[\phi])}), \quad (8)$$

$$\langle \phi \rangle = \frac{1}{Z} \int D\phi (\phi e^{-(\mathcal{H}_b[\phi] + \mathcal{H}_s[\phi])}). \quad (9)$$

In the present work we shall provide general scaling properties with the quantitative results for the scaling functions determined within mean field approximation, i.e., only the order parameter profile  $m(z)$  with the maximum statistical weight will be considered and all others will be neglected:

$$\left. \frac{\delta \mathcal{H}[\phi]}{\delta \phi} \right|_{\phi=m} = 0. \quad (10)$$

This mean field approximation is valid above the upper critical dimension  $d_c = 4$ . Within this approximation the aforementioned critical exponents take the following values:

$$\beta(d \geq 4) = \frac{1}{2} \quad \text{and} \quad \nu(d \geq 4) = \frac{1}{2}, \quad (11)$$

whereas the critical exponents at physical dimension  $d = 3$  are [42]

$$\beta(d = 3) = 0.3265 \quad \text{and} \quad \nu(d = 3) = 0.6305. \quad (12)$$

The mean field approximation is important because it is the zeroth-order approximation in a systematic Feynman graph expansion on which the ( $\epsilon = d - 4$ ) expansion and hence the renormalization group approach are based [6,31,43]. The higher orders in the Feynman graph expansion require integrations over the mean field order parameter profile and the two-point correlation function [compare Eq. (3.209) in Ref. [31]] which can be carried out reasonably if they are available in an analytical form. However, the mean field approximation is expected to yield the qualitatively correct behavior of the scaling functions if for the variables forming the scaling variables the correct critical exponents are used, which are known with high accuracy [42] [see Eq. (12)].

Taking the functional derivative of the Hamiltonian with respect to the order parameter [see Eqs. (6), (7), and (10)] yields a differential equation for the mean field profile  $m(z)$  of the order parameter [30,31],

$$-\frac{\partial^2}{\partial z^2} m + \pi m + \frac{u}{3!} m^3 = 0, \quad (13)$$

with boundary conditions

$$\left. \frac{\partial m}{\partial z} \right|_{z=0} = cm(z=0) - h_1 \quad (14)$$

and

$$\left. \frac{\partial m}{\partial z} \right|_{z \rightarrow \infty} = 0. \quad (15)$$

### A. Infinite surface fields

For systems that belong to the extraordinary surface universality class ( $h_1 = 0, c < 0$ ) the boundary condition at the surface (14) simplifies and the differential equation (13) has an analytical solution [31]. Together with the scaling behavior of the order parameter (1) and the nonuniversal amplitude  $a$  which within the present model and within mean field (MF) approximation equals  $a = (6/u)^{1/2} (\xi_0^+)^{-1}$  this leads to scaling functions  $P_{\text{MF}}^{\pm}(w)$  of the following form:

$$P_{\text{MF}}^+(w) = \frac{\sqrt{2}}{\sinh(w + w_0)}, \quad \coth(w_0) = |\tilde{c}|, \quad (16)$$

$$P_{\text{MF}}^-(w) = \coth\left(\frac{w + w_0}{2}\right), \quad \sinh(w_0) = \frac{1}{|\tilde{c}|}, \quad (17)$$

where  $\tilde{c} = \xi_0^+ |t|^{-1/2} c$  is the scaled and dimensionless surface enhancement. The parameter  $w_0$  vanishes at the extraordinary fixed point ( $\tilde{h}_1 = 0, \tilde{c} \rightarrow -\infty$ )—with the scaled and dimensionless surface field  $\tilde{h}_1 = (u/6)^{1/2} \xi_0^{+2} |t|^{-1} h_1$ —so that Eqs. (16) and (17) reduce to the scaling functions

$$P_{\infty}^+(w) = \frac{\sqrt{2}}{\sinh(w)} \quad (18)$$

and

$$P_{\infty}^-(w) = \coth\left(\frac{w}{2}\right), \quad (19)$$

which in the following are referred to as “half-space profiles” above and below the critical temperature, respectively. As already mentioned at the beginning of Sec. II the extraordinary fixed point is equivalent to the normal fixed point ( $|\tilde{h}_1| \rightarrow \infty, \tilde{c} = 0$ ) and thus Eqs. (18) and (19) represent the latter fixed point as well.

### B. Finite surface fields

Since in experimental systems the surface fields are finite, we also discuss the case of a homogeneous substrate with a surface field  $0 < h_1 < \infty$ . This provides the starting point for discussing the case of a chemical step with finite—albeit strong—surface fields that we shall consider in Sec. III A 2. Off criticality (i.e.,  $t \neq 0$ ) and for a finite surface field  $h_1$  the scaled surface field  $\tilde{h}_1 = (u/6)^{1/2} \xi_0^{+2} |t|^{-1} h_1$  is also finite. At the substrate, for finite surface fields the order parameter profiles  $P_{h_1}^{\pm}(w)$  above and below the critical temperature have finite values  $P_{h_1}^+(w=0) = P_{\text{sub}}^+$  and  $P_{h_1}^-(w=0) = P_{\text{sub}}^-$ , respectively.

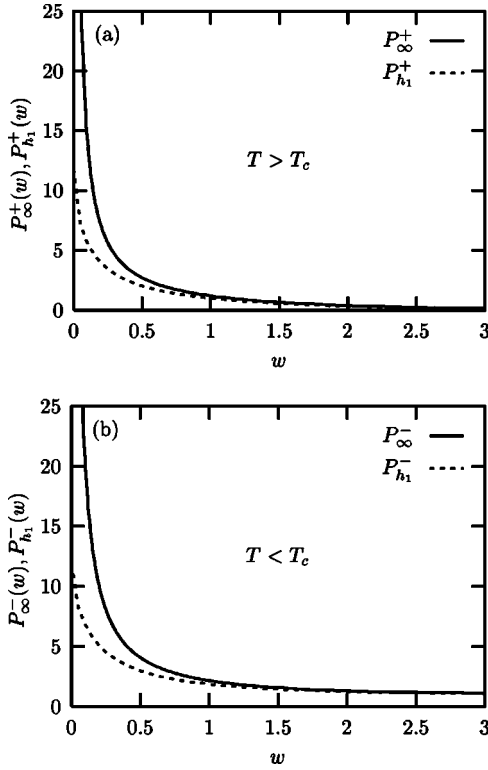


FIG. 2. (a) The half-space profile  $P_{\infty}^{+}(w=z/\xi^{+})$  for an infinite surface field  $\tilde{h}_1$  and  $P_{h_1}^{+}(w=z/\xi^{+})$  for a finite scaled surface field  $\tilde{h}_1=100$  above the critical temperature. (b) The same below  $T_c$  with  $w=z/\xi^{-}$ .

These values are determined by the following equations, which are obtained by performing the first integral of the differential equations for  $P_{MF}^{+}$  and  $P_{MF}^{-}$ , corresponding to Eq. (13) [30]:

$$P_{\text{sub}}^{+4} + 2(1 - \tilde{c}^2)P_{\text{sub}}^{+2} + 4\tilde{c}\tilde{h}_1P_{\text{sub}}^{+} - 2\tilde{h}_1^2 = 0 \quad (20)$$

and

$$P_{\text{sub}}^{-4} - 2(1 + 2\tilde{c}^2)P_{\text{sub}}^{-2} + 4\tilde{c}\tilde{h}_1P_{\text{sub}}^{-} - 2\tilde{h}_1^2 + 1 = 0. \quad (21)$$

For the normal surface universality class (i.e.,  $\tilde{c}=0$ ) Eqs. (20) and (21) simplify and we find for the order parameter  $P_{\text{sub}}^{+}$  and  $P_{\text{sub}}^{-}$  at the substrate above and below the critical temperature, respectively,

$$P_{\text{sub}}^{+} = \pm \sqrt{\sqrt{1 + 2\tilde{h}_1^2} - 1}, \quad \tilde{h}_1 \geq 0, \quad (22)$$

and

$$P_{\text{sub}}^{-} = \pm \sqrt{\sqrt{2\tilde{h}_1^2} + 1}, \quad \tilde{h}_1 \geq 0. \quad (23)$$

Using these equations together with the boundary condition (14) and the differential equation (13) the half-space profile for finite surface fields  $P_{h_1}^{\pm}(w)=P^{\pm}(w, \tilde{h}_1 < \infty, \tilde{c}=0)$  can be calculated numerically (see the Appendix). In Fig. 2 the half-space profiles for infinite and finite surface fields are shown for temperatures above as well as below the critical temperature. In the following section we shall consider inho-

mogeneous substrates, i.e., substrates with a laterally varying surface field  $h_1$  for which further length scales come into play, which also scale with the correlation length  $\xi^{\pm}$ .

### III. CRITICAL ADSORPTION AT INHOMOGENEOUS SUBSTRATES

#### A. Chemical step

First we consider an infinite substrate which is divided into two halves with opposing surface fields  $h_1$  so that there is a chemical step at the straight contact line ( $x=z=0$ ) of the two halves [see Fig. 1(a)]. We introduce the scaled coordinates  $v=x/\xi$  and  $w=z/\xi$  describing the distance  $x$  from the contact line and  $z$  from the substrate, respectively, in units of the correlation length  $\xi$ . The system is translationally invariant in the direction perpendicular to the  $x$ - $z$  plane.

For laterally inhomogeneous systems one has to reconsider whether the surface Hamiltonian  $\mathcal{H}_s$  [Eq. (7)] should contain terms like  $\phi\partial_{\parallel}\phi$  and  $\phi\partial_{\perp}\phi$ . However, the term  $\phi\partial_{\parallel}\phi$  would favor order parameter profiles which are nonsymmetric with respect to  $(x=0, y)$  even without surface fields. Therefore such a term is ruled out. The term  $\phi\partial_{\perp}\phi$  leads only to a redefinition of the surface enhancement [31] and therefore can be neglected for homogeneous as well as for the inhomogeneous substrates. Thus the surface Hamiltonian  $\mathcal{H}_s$  for inhomogeneous surface fields has the same form as the one for homogeneous surface fields [Eq. (7)].

#### 1. Infinite surface fields

First we analyze the case of a homogeneous infinite surface field on both halves of the substrate but with opposite sign and a vanishing surface enhancement, i.e., we consider a steplike lateral variation of the surface field  $h_1$ :  $h_1 = \pm\infty$  for  $x \geq 0$ . The actual smooth variation of  $h_1$  on a microscopic scale turns effectively into a steplike variation if considered on the scale  $\xi^{\pm}$ .

*a. Order parameter profiles.* The order parameter profile for a system with a chemical step (CS) exhibits the following scaling property:

$$\phi(x, z, t) = a|t|^{\beta}P_{\text{CS}}^{\pm}\left(v = \frac{x}{\xi^{\pm}}, w = \frac{z}{\xi^{\pm}}\right) \quad \text{for } t \geq 0, \quad (24)$$

which generalizes Eq. (1). This scaling function shows the following limiting behavior. For large distances from the chemical step ( $|v| \rightarrow \infty$ ) the profile approaches the corresponding order parameter profile of a system with a homogeneous substrate, whose asymptotic behavior is given by Eqs. (2)–(4),  $P_{\text{CS}}^{\pm}(|v| \rightarrow \infty, w) = P_{\infty}^{\pm}(w)$ . For large distances from the substrate ( $w \rightarrow \infty$ ) and above the critical temperature the order parameter profile vanishes for all values of  $v$ , i.e.,  $P_{\text{CS}}^{+}(v, w \rightarrow \infty) = 0$  while below the critical temperature the order parameter profile tends to the profile  $P_{\text{LV}}^{-}(v)$  of a free liquid-vapor interface  $P_{\text{CS}}^{-}(v, w \rightarrow \infty) = P_{\text{LV}}^{-}(v)$  [44]. The mean field approximation to this profile is given by

$$P_{\text{LV}}^{-}(v) = \tanh\left(\frac{v}{2}\right). \quad (25)$$

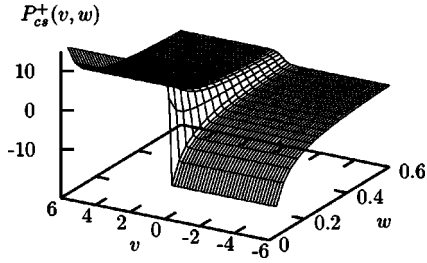


FIG. 3. Scaling function  $P_{CS}^+(v=x/\xi^+, w=z/\xi^+)$  for the order parameter profile of a system above the critical temperature and confined by a substrate with a chemical step located at  $x=z=0$ . Due to symmetry  $P_{CS}^+(v=0, w)=0$ .

Figure 3 provides a three-dimensional plot of the numerically determined (see the Appendix) order parameter profile for  $T > T_c$ . In Fig. 4 we show cuts through the order parameter profile parallel to the substrate as it changes with increasing distance from the substrate. In order to provide a clearer comparison the cross sections are normalized to 1 at the lateral boundaries via dividing by the exponentially decaying half-space profile  $P_\infty^\pm(w)$ . From the fact that the cross sections do not fall onto one curve follows that the scaling

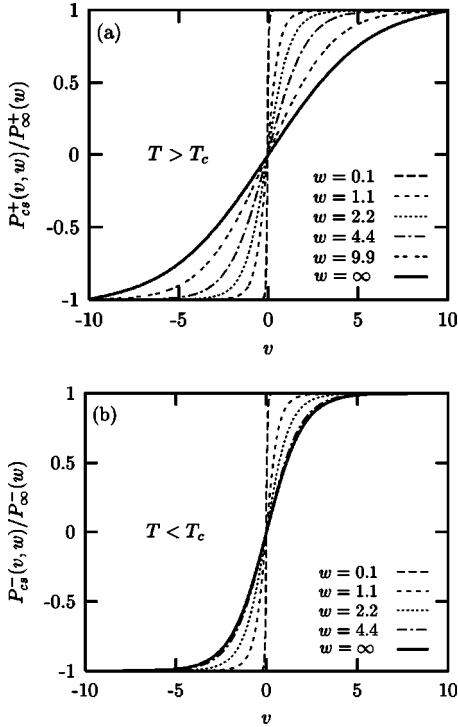


FIG. 4. Cuts through the order parameter profiles  $P_{CS}^+(v, w)$ , as shown in Fig. 3, and  $P_{CS}^-(v, w)$  for  $w=z/\xi^\pm=\text{const}$  with the normalization  $P_{CS}^\pm(v, w)/P_\infty^\pm(w)$  (a) above and (b) below the critical temperature. Upon increasing the distance from the substrate the slope of the curves at  $v=0$  decreases. The solid lines represent the limiting curves for  $w \rightarrow \infty$ . (a) Above the critical temperature the limiting slope at  $v=0$  of the normalized curves is given by  $s^+(w \rightarrow \infty)/P_\infty^+(w \rightarrow \infty) = A_2^+/(2\sqrt{2}) \approx 0.200$  with the slope  $s^+(w) = [\partial P_{CS}^+(v, w)/\partial v]_{v=0}$  of the unnormalized scaling function and its amplitude  $A_2^+ = 0.566$  [see, Eq. (28) and Fig. 5]. (b) Below  $T_c$  the limiting curve corresponds to  $\tanh(v/2)$ .

function  $P_{CS}^\pm(v, w)$  does not separate into a  $v$ -dependent and a  $w$ -dependent part. It shows that the slope  $s^\pm(w) = [\partial P_{CS}^\pm(v, w)/\partial v]_{v=0}$  of the scaling function at the step decreases with increasing distance from the substrate which visualizes the healing of the frustration upon approaching the bulk. Note that the slopes in Fig. 4 must be multiplied by  $P_\infty^\pm(w)$  in order to obtain  $s^\pm(w)$ . From Eq. (24) it follows that

$$\left. \frac{\partial \phi(x, z, t)}{\partial x} \right|_{x=0} = a \frac{|t|^\beta}{\xi} \left. \frac{\partial P_{CS}^\pm(v, w)}{\partial v} \right|_{v=0} = \frac{a}{\xi_0^\pm} |t|^{\beta+\nu} s^\pm(w). \quad (26)$$

Since there is a nonvanishing order parameter profile even at the critical point [ $\phi(x, z, t=0) \neq 0$ ] the overall temperature dependence of the slope  $\partial \phi/\partial x$  in Eq. (26) has to vanish. Therefore one finds for  $w = (z/\xi_0^\pm)t^\nu \rightarrow 0$ :

$$s^\pm(w \rightarrow 0) = A_1^\pm w^{-\beta/\nu-1}. \quad (27)$$

For  $T > T_c$  the slope  $s^+(w)$  vanishes exponentially upon approaching the bulk:

$$s^+(w \rightarrow \infty) = A_2^+ e^{-w}. \quad (28)$$

Below  $T_c$  the slope  $s^-(w \rightarrow \infty)$  approaches the slope  $s_{LV} = [\partial P_{LV}^-(v)/\partial v]_{v=0}$  of the scaling function for the liquid-vapor profile [Eq. (25)] at most  $\sim e^{-w}$  or slower:

$$s^-(w \rightarrow \infty) - s_{LV} = A_2^- e^{-Cw}, \quad 0 < C \leq 1. \quad (29)$$

As the half-space profiles  $P_{CS}^+(v \rightarrow \pm\infty, w) = \pm P_\infty^+(w)$  [Eq. (3)] and  $P_{CS}^-(v \rightarrow \pm\infty, w) = \pm P_\infty^-(w)$  [Eq. (4)] decay exponentially  $\sim e^{-w}$  for large distances from the substrate, the slope  $s^\pm(w)$  cannot decay faster because this would require that the slope  $s^\pm(w)$  be smaller than the slope  $(\partial P_{CS}^\pm/\partial v)_{v_0}$  for a certain  $v_0 \neq 0$ . On the other hand a decay of the slope  $s^+(w)$  slower than  $e^{-w}$  would lead to an unphysical increasing slope of the normalized cross sections at  $v=0$  with increasing distance from the substrate. However, for the slope  $s^-(w)$  a decay toward  $s_{LV}$  slower than  $\sim e^{-w}$  cannot be ruled out.

Within mean field theory Eqs. (25) and (27) yield  $s^\pm(w \rightarrow 0) \sim w^{-2}$  [see also Eq. (11)] and  $s^-(w \rightarrow \infty) = s_{LV} = \frac{1}{2}$ , respectively, which is in agreement with the numerical results shown in Fig. 5. These results for the slope  $s^\pm(w)$  of the scaled order parameter profile  $P_{CS}^\pm(v, w)$  transform into the following findings for the slope of the unscaled order parameter profile  $\phi(x, z)$ :

$$\left. \frac{\partial \phi}{\partial x} \right|_{x=0} \sim z^{-\beta/\nu-1}, \quad T = T_c, \quad (30)$$

$$\left. \frac{\partial \phi}{\partial x} \right|_{x=0} \sim |t|^{\beta+\nu} e^{-z/\xi^\pm}, \quad T > T_c, \quad z \gg \xi^\pm, \\ \sim (\xi^\pm)^{-\beta/\nu-1} e^{-z/\xi^\pm}, \quad (31)$$

and

$$\left. \frac{\partial \phi}{\partial x} \right|_{x=0} - \frac{\partial \phi_{lv}}{\partial x} \sim |t|^{\beta+\nu} e^{-Cz/\xi^-}, \quad T < T_c, \quad z \gg \xi^+, \\ \sim |\xi^-|^{-\beta/\nu-1} e^{-Cz/\xi^-}. \quad (32)$$

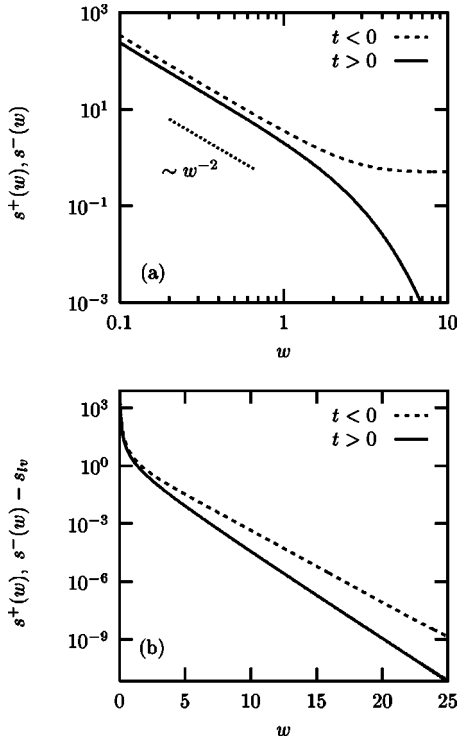


FIG. 5. Slopes  $s^\pm(w)$  at the chemical step of the scaling functions  $P_{CS}^\pm(v=x/\xi^\pm, w=z/\xi^\pm)$  for the order parameter profile of a system with a chemical step at  $x=0$ . (a) For small distances from the substrate the slopes diverge as  $A_1^\pm w^{-2}$  with amplitudes  $A_1^+=2.367\pm 0.006$  and  $A_1^-=3.366\pm 0.005$  [see Eq. (27)]. (b) For large distances the slopes decay exponentially, above  $T_c$ ,  $s^+(w\rightarrow\infty)=A_2^+e^{-w}$  with  $A_2^+=0.566\pm 0.001$  [see Eq. (28)]; below  $T_c$ ,  $s^-(w\rightarrow\infty)$  approaches its limiting value  $s_{LV}=1/2$  more slowly, i.e., as  $A_2^-e^{-Cw}$  with  $A_2^-=2.338\pm 0.001$  and  $C=0.858\pm 0.001$  [see Eq. (29)].

As an example we investigate more closely the healing effect above the critical temperature. To this end we rescale the normalized cross sections of Fig. 4 such that their slope at  $v=0$  becomes 1; see Fig. 6. It shows that these rescaled normalized cross sections for different distances from the substrate differ basically only in the region where the curvature of these curves is largest. From the fact that these cross sections do not fall onto one curve it follows that the scaling function  $P^\pm(v, w)$  is not simply given by the knowledge of

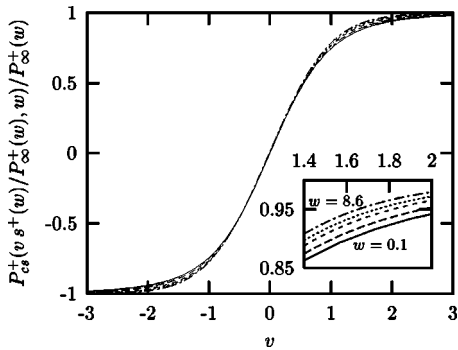


FIG. 6. Rescaled normalized cross sections with slope 1 at  $v=0$  for  $w=0.1, 1.5, 2.9, 4.3, 8.6$ .

one cross section, the slope  $s(w)$ , and the half-space profile  $P_\infty^\pm(w)$ , but requires the full numerical analysis. Nonetheless Fig. 6 demonstrates that to a large extent the rescaling used there reduces the full scaling function  $P_{CS}^\pm(v, w)$  to a single function of  $v$  only.

*b. Excess adsorption.* It is a challenge to determine experimentally the full order parameter profile  $\phi(x, z)$ . Therefore in the following we analyze the adsorption  $\Gamma = \int dV \phi(\mathbf{r})$  at the substrate which as an integral quantity is more easily accessible to experiments. To this end for any system with an order parameter profile  $\phi(x, z)$  and a corresponding scaling function  $P^\pm(v, w)$  we introduce a suitable reference system with an order parameter profile  $\phi_{\text{ref}}(x, z)$  and the corresponding scaling function  $P_{\text{ref}}^\pm(v, w)$ . This allows us to introduce an excess adsorption  $\Gamma_{\text{ex}}$  with respect to this reference system,

$$\Gamma_{\text{ex}} = H \int \int dx dz [\phi(x, z) - \phi_{\text{ref}}(x, z)] = a|t|^\beta \xi_0^{\pm 2} H \tilde{\Gamma}_{\text{ex}}^\pm \quad (33)$$

with its universal part  $\tilde{\Gamma}_{\text{ex}}^\pm$  defined as [see Eqs. (1) and (24)]

$$\tilde{\Gamma}_{\text{ex}}^\pm = \int \int dv dw [P^\pm(v, w) - P_{\text{ref}}^\pm(v, w)]. \quad (34)$$

$H$  denotes the extension of the system perpendicular to the  $x$ - $z$  plane. [In the three-dimensional case  $H$  corresponds to the one-dimensional extension of the system in the  $y$  direction. Within mean field theory, which is valid for dimensions  $d \geq 4$ ,  $H$  corresponds to the  $(d-2)$ -dimensional extension of the system in the  $y_1, \dots, y_{d-2}$  directions.] Equation (33) leads to the following temperature dependence of the excess adsorption:

$$\Gamma_{\text{ex}} = \tilde{\Gamma}_{\text{ex}}^\pm a \xi_0^{\pm 2} H |t|^{\beta-2\nu}, \quad (35)$$

with the universal amplitude  $\tilde{\Gamma}_{\text{ex}}^\pm$  and three nonuniversal amplitudes  $a$ ,  $\xi_0^\pm$ , and  $H$ . Within mean field approximation this yields  $\Gamma_{\text{ex}} = \tilde{\Gamma}_{\text{ex}}^\pm a \xi_0^{\pm 2} H |t|^{-1/2}$ . For our choices of reference systems as given below  $P_{\text{ref}}^\pm(v, w)$  leads even within mean field theory to a cancellation of the divergence of the corresponding integrals over the scaling function  $P^\pm(v, w)$  caused by small distances from the substrate. This way the numerical mean field data for  $d=4$  allow one to make meaningful approximate contact with potential experimental data for  $d=3$ .

Specifically, for the chemical step we introduce a reference system  $P_{CS,0}^\pm(v, w)$  which can be interpreted as a system with a chemical step for which no healing at the chemical step occurs:

$$P_{CS,0}^\pm(v, w) = \begin{cases} -P_\infty^\pm(w), & v < 0, \\ +P_\infty^\pm(w), & v > 0. \end{cases} \quad (36)$$

Since this choice of the reference systems leads to a vanishing excess adsorption for any antisymmetric (with respect to  $v=0$ ) scaling function  $P_{CS}^\pm(v, w)$  upon integration over the whole half space  $w > 0$ , we restrict the integration to a quarter of the space (see Fig. 7):

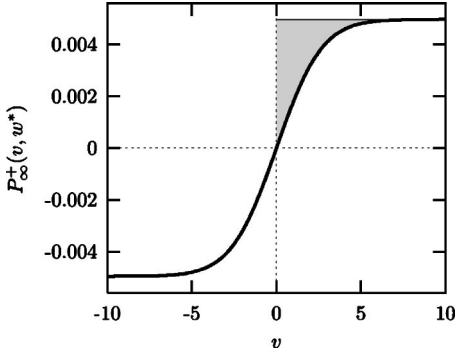


FIG. 7. The shaded area indicates the contribution to the excess adsorption  $\tilde{\Gamma}_{\text{ex,CS}}^{\pm}$  as defined in Eq. (37) for  $w=w^*=6.0$  for a system above  $T_c$  and with a chemical step.  $\tilde{\Gamma}_{\text{ex,CS}}^{\pm}$  is obtained by summing these shaded areas over  $w$ .

$$\tilde{\Gamma}_{\text{ex,CS}}^{\pm} = \int_0^{\infty} dv \int_0^{\infty} dw [P_{\text{CS}}^{\pm}(v, w) - P_{\text{CS},0}^{\pm}(v, w)]. \quad (37)$$

For a binary liquid mixture confined by a substrate with a chemical step  $\tilde{\Gamma}_{\text{ex,CS}}^{\pm}$  can be interpreted as the amount of particles of one type removed across the chemical step from the substrate that prefers them.

Below  $T_c$  the scaling function  $P_{\text{LV}}^-(v) = P_{\text{CS}}^-(v, w = \infty)$  [Eq. (25)] of the liquid-vapor profile gives rise to a nonvanishing universal excess adsorption  $\tilde{\Gamma}_b^-$  with respect to the chosen reference system  $P_{\text{CS},0}^-$ :

$$\begin{aligned} \tilde{\Gamma}_b^- &= \int_0^{\infty} dv [P_{\text{LV}}^-(v) - P_{\text{CS},0}^-(v, w = \infty)] = \int_0^{\infty} dv [P_{\text{LV}}^-(v) - 1] \\ &= -2 \ln 2. \end{aligned} \quad (38)$$

Thus  $\tilde{\Gamma}_{\text{ex,CS}}^-$  can be written as

$$\tilde{\Gamma}_{\text{ex,CS}}^- = \tilde{L} \tilde{\Gamma}_b^- + \tilde{\Gamma}_{\text{ex},f}^- \quad (39)$$

where  $\tilde{L} = L/\xi^- \rightarrow \infty$  denotes the extension of the system perpendicular to the substrate and the system-size-independent contribution  $\tilde{\Gamma}_{\text{ex},f}^-$  characterizes the influence of the chemical step. From our numerical analysis we find the following universal excess adsorption amplitudes:

$$\tilde{\Gamma}_{\text{ex,CS}}^+ = -1.457 \pm 0.001, \quad (40)$$

$$\tilde{\Gamma}_{\text{ex},f}^- = 1.299 \pm 0.001. \quad (41)$$

## 2. Nonantisymmetric finite surface fields

Next we study an infinite substrate consisting of two halves with surface fields of opposite sign but different absolute finite values  $h_p$  and  $h_n$ , respectively, and a vanishing surface enhancement. As before we consider a steplike variation of the surface field  $h_1$ :

$$h_1(x) = \begin{cases} h_n, & x < 0, \\ h_p, & x > 0. \end{cases} \quad (42)$$

The absence of antisymmetry for these systems is reflected by the “zero line”  $v_0(w)$ , where the order parameter vanishes:  $P(v_0, w) = 0$ . For ratios  $-\tilde{h}_p/\tilde{h}_n \neq 1$  of the scaled surface fields (see Sec. II B) the zero line is shifted toward the region of the surface field with the smaller absolute value. Furthermore the zero line is not straight, but tends to increasing values  $|v_0|$  for increasing distance  $w$  from the substrate. However, the deviation of the zero line from the line  $(v=0, w)$  decreases for  $-\tilde{h}_p/\tilde{h}_n \rightarrow 1$ . For constant ratios  $-\tilde{h}_p/\tilde{h}_n$  the deviation of the zero line from the line  $(v=0, w)$  decreases with increasing absolute values of the scaled surface fields  $\tilde{h}_p$  and  $\tilde{h}_n$ . These results demonstrate how the order parameter structure for the fixed point fields  $|\tilde{h}_p|, |\tilde{h}_n| \rightarrow \infty$  emerges smoothly from the general case of finite fields. In this sense in the following we focus on the case of infinite surface fields, i.e., strong adsorption.

## B. Single stripe

The second system we focus on consists of a laterally extended substrate with a negative surface field  $h_1 \rightarrow -\infty$  in which a stripe of width  $S$  with a positive surface field  $h_1 \rightarrow \infty$  is embedded [see Fig. 1(b)]. The surface field  $h_1$  is assumed to vary in a steplike way:

$$h_1(x) = \begin{cases} +\infty, & x \in [0, S], \\ -\infty, & x \notin [0, S]. \end{cases} \quad (43)$$

We introduce the coordinates  $v$  and  $w$  scaled in units of the correlation length, where  $v$  denotes the scaled distance from the left border of the stripe at  $x=0$  and  $w$  the scaled distance from the substrate. The influence of the stripe width  $S$  and of the reduced temperature  $t$  are captured by the scaled stripe width  $\tilde{S} = S/\xi^{\pm}$ . The order parameter profile for the system with a single stripe (SS) exhibits the scaling property

$$\phi(x, z, t, S) = a |t|^\beta P_{\text{SS}}^{\pm} \left( v = \frac{x}{\xi^{\pm}}, w = \frac{z}{\xi^{\pm}}, \tilde{S} = \frac{S}{\xi^{\pm}} \right) \quad (44)$$

with the limiting behavior

$$P_{\text{SS}}^{\pm}(v, w, \tilde{S} = 0) = -P_{\infty}^{\pm}(w), \quad (45)$$

$$P_{\text{SS}}^{\pm}(v, w, \tilde{S} \rightarrow \infty) = P_{\text{CS}}^{\pm}(v, w). \quad (46)$$

Figures 8(a) and 8(b) show cross sections (parallel to the substrate) through the order parameter scaling function  $P_{\text{SS}}^{\pm}(v, w, \tilde{S})$  for systems with different scaled stripe width  $\tilde{S}$  at two different scaled distances  $w$  from the substrate in comparison with a cross section through the order parameter profile  $P_{\text{CS}}^{\pm}(v, w)$  at a single chemical step at  $v=0$  (see Sec. III A). With increasing scaled width  $\tilde{S} \rightarrow \infty$  of the stripe the left part of the cross section of the stripe system merges with the cross section of the system with a single step. Further away from the substrate the mutual influence of the two step



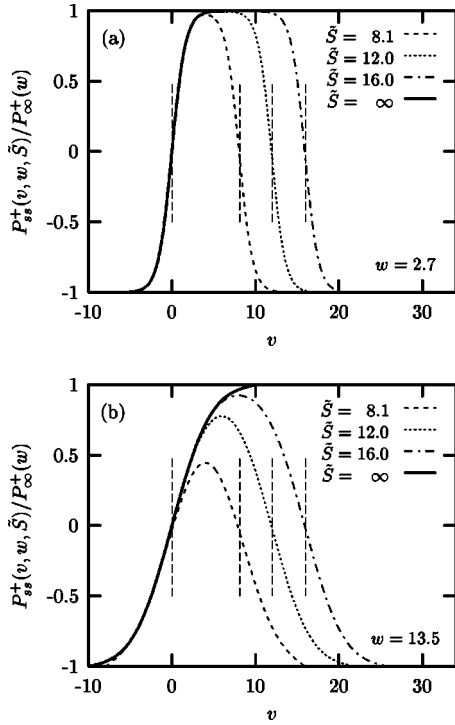


FIG. 8. Comparison between the normalized cross sections of the order parameter scaling function near a substrate with negative surface field in which a stripe with positive surface field of scaled width  $\tilde{S}$  is embedded and the normalized cross sections of the order parameter profile near a single chemical step (which emerges as limiting case for  $\tilde{S} \rightarrow \infty$ ), (a) at a scaled normal distance  $w=2.7$ , and (b) at  $w=13.5$ . Here we consider the case  $T > T_c$ . The chemical steps are located at  $x=0$  and  $x=S$  corresponding to  $v=0$  and  $v=\tilde{S}$  (see vertical lines).

structures onto each other is more pronounced [see Fig. 8(b)] and stronger for smaller stripes.

For systems with a single chemical stripe on the substrate a reference system with the scaling function  $P_{SS,0}^+(v, w, \tilde{S})$  can be introduced, similar to the one for a single chemical step, which can be interpreted as a system with a single chemical stripe on the substrate where no healing occurs:

$$P_{SS,0}^+(v, w, \tilde{S}) = \begin{cases} +P_{\infty}^+(w), & v \in [0, \tilde{S}], \\ -P_{\infty}^+(w), & v \notin [0, \tilde{S}]. \end{cases} \quad (47)$$

This reference system allows us to define the excess adsorption  $\tilde{\Gamma}_{\text{ex,SS}}^+$  for the striped systems:

$$\tilde{\Gamma}_{\text{ex,SS}}^+(\tilde{S}) = \int_{-\infty}^{\infty} dv \int_0^{\infty} dw [P_{SS}^+(v, w, \tilde{S}) - P_{SS,0}^+(v, w, \tilde{S})]. \quad (48)$$

Equation (48) can be rewritten as

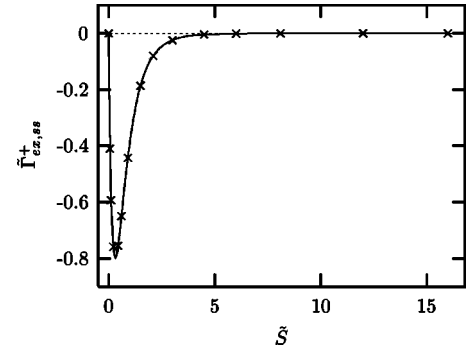


FIG. 9. Universal excess adsorption  $\tilde{\Gamma}_{\text{ex,SS}}^+$  [Eq. (48)] for a single stripe with respect to a system with no healing as a function of the stripe width  $\tilde{S}$ . For  $\tilde{S}=0$  the system corresponds to a system with a homogeneous substrate whose corresponding excess adsorption is 0. In the limit  $\tilde{S} \rightarrow \infty$  the stripe system corresponds to two independent chemical steps whose excess adsorption also vanishes due to antisymmetry of the profiles around  $v=0$  and  $v=\tilde{S} \rightarrow \infty$ . The non-vanishing excess adsorption for intermediate stripe widths  $\tilde{S}$  indicates the effect of the stripe with a surface field opposite to the one of the embedding substrate.  $\tilde{\Gamma}_{\text{ex,SS}}^+$  attains its minimum at  $\tilde{S} \approx 0.3$ .

$$\tilde{\Gamma}_{\text{ex,SS}}^+(\tilde{S}) = \lim_{\tilde{B} \rightarrow \infty} \left\{ \int_{-(\tilde{B}-\tilde{S})/2}^{(\tilde{B}+\tilde{S})/2} dv \int_0^{\infty} dw [P_{SS}^+(v, w, \tilde{S}) + (\tilde{B} - 2\tilde{S})\tilde{\Gamma}_{\infty}^+] \right\}, \quad (49)$$

where  $B = \tilde{B}\xi \gg S$  is the overall lateral extension of the substrate surface in the  $x$  direction [see Fig. 1(b)] and  $\tilde{\Gamma}_{\infty}^+ = \int_0^{\infty} dw P_{\infty}^+(w)$  is a universal number characterizing the amplitude of the excess adsorption at a *homogenous* substrate:  $\int_0^{\infty} dz \phi(z, t) = \tilde{\Gamma}_{\infty}^+ a \xi_0^+ t t^{\beta-\nu}$ . The value of  $\tilde{\Gamma}_{\infty}^+$  is discussed in Ref. [33] and in Ref. [25] where it is denoted as  $\tilde{\Gamma}_{\infty}^+ = g_+ / (\nu - \beta)$  [see Eq. (2.9) and Fig. 5 in Ref. [25]; in  $d=3$  one has  $\tilde{\Gamma}_{\infty}^+ = 2.27$ ]. Equation (49) describes how in an operational sense the universal function  $\tilde{\Gamma}_{\text{ex,SS}}^+(\tilde{S})$  (see Fig. 9) can be obtained from the measurements of the excess adsorption (relative to the bulk order parameter) at a striped surface and from those of the excess adsorption at the corresponding homogeneous surface.

Figure 9 shows the dependence of the excess adsorption  $\tilde{\Gamma}_{\text{ex,SS}}^+$  on the scaled stripe width  $\tilde{S}$ . For  $\tilde{S} \rightarrow \infty$  the structures associated with the two chemical steps forming the stripe decouple so that  $\tilde{\Gamma}_{\text{ex,SS}}^+(\tilde{S} \rightarrow \infty) = 0$ . Upon construction  $\tilde{\Gamma}_{\text{ex,SS}}^+(\tilde{S}=0) = 0$ . The decrease of the excess adsorption at  $\tilde{S} \approx 1$  arises due to the fact that for sufficiently small stripes the spatial region where the order parameter profile is positive no longer resembles a rectangular but a tonguelike shape (see Fig. 10). Since for the reference system the region with a positive order parameter still resembles a rectangle this leads to a negative excess adsorption.

For different stripe width  $\tilde{S}$  the tonguelike regions defined by the zero lines  $v_0(w)$  where the order parameter vanishes,

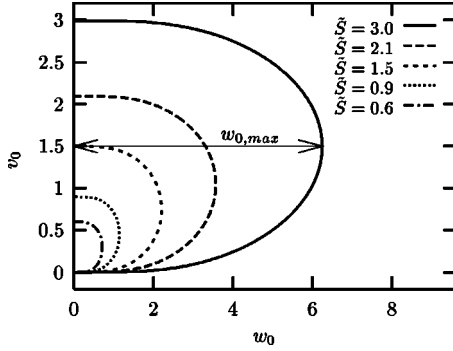


FIG. 10. Zero lines  $v_0(w)$  where the order parameter vanishes,  $P(v_0, w) = 0$ , for different stripe widths  $\tilde{S}$ . Outside the tongue the order parameter is negative, corresponding to the preference for the substrate outside the stripe. Inside the tongue the order parameter is positive and thus demarcates the range of influence of the stripe with opposite preference.

$P(v_0, w) = 0$ , are shown in Fig. 10. The width of the tongue at the substrate is given by the stripe width  $\tilde{S}$  due to the infinitely strong surface fields. With increasing stripe width  $\tilde{S}$  the tongue becomes longer. Figure 11 shows the dependence of the length  $w_{0,max}$  of the tongue on the stripe width  $\tilde{S}$ . It shows that for small stripes  $w_{0,max}$  increases linearly with  $\tilde{S}$ .

### C. Periodic stripes

As a natural extension we now consider a substrate with a periodic array of stripes with alternating surface fields [see Fig. 1(c)]: stripes of width  $S_p(S_n)$  with positive (negative) surface field  $h_1 \rightarrow \infty (h_1 \rightarrow -\infty)$ . In the lateral  $x$  direction we employ periodic boundary conditions. The corresponding scaling function  $P_{PS}$  for the order parameter distribution near the substrate with periodic stripes (PS) depends on two scaled coordinates  $v = x/\xi^+$  and  $w = z/\xi^+$  and on two scaled stripe widths  $\tilde{S}_p = S_p/\xi^+$  and  $\tilde{S}_n = S_n/\xi^+$  or, equivalently,  $\tilde{S}_p$  and  $\tilde{S}_n/\tilde{S}_p = S_n/S_p$ . Thus in the series  $P_\infty$ ,  $P_{CS}$ ,  $P_{SS}$ , and  $P_{PS}$  each scaling function acquires one additional scaling variable. Considering the excess adsorption  $\tilde{\Gamma}_{ex,PS}^+(\tilde{S}_p, \tilde{S}_n/\tilde{S}_p)$  re-

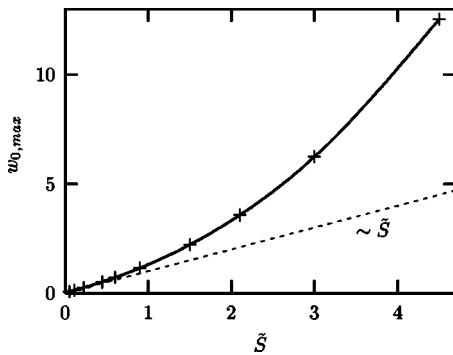


FIG. 11. Dependence of the length  $w_{0,max}$  of the tongues shown in Fig. 10 on the stripe width  $\tilde{S}$ . For small stripe widths the length of the tongue increases linearly; with increasing stripe widths  $\tilde{S}$  the length  $w_{0,max}$  of the tongues diverges.

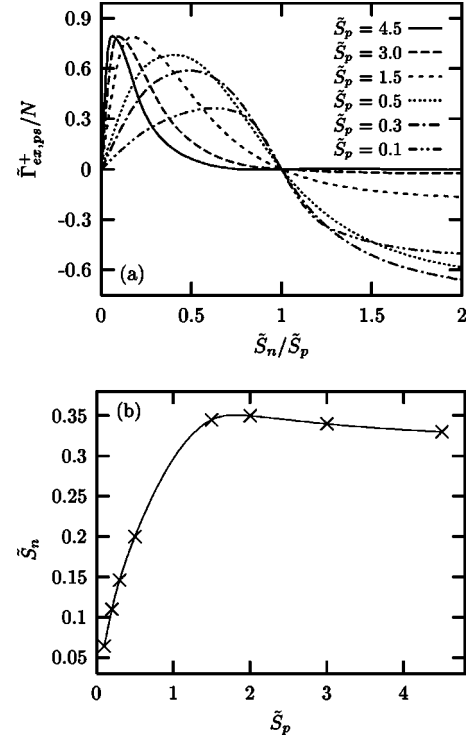


FIG. 12. (a) Universal scaling function for the excess adsorption  $\tilde{\Gamma}_{ex,PS}^+$  per unit cell [Eqs. (50) and (51)] for a system with a periodic stripe pattern of negative and positive surface fields with scaled widths  $\tilde{S}_n = S_n/\xi$  and  $\tilde{S}_p = S_p/\xi$ , respectively. The case  $\tilde{S}_n/\tilde{S}_p = 0$  corresponds to a homogeneous substrate with a positive surface field. The excess adsorption vanishes for  $\tilde{S}_n = \tilde{S}_p$  due to symmetry reasons. For large ratios  $\tilde{S}_n/\tilde{S}_p$  with  $\tilde{S}_p$  fixed the excess adsorption  $\tilde{\Gamma}_{ex,PS}^+/N$  tends to the excess adsorption of a single stripe of width  $\tilde{S}_p$  that is given by Fig. 9. (b) Loci of the maxima of  $\tilde{\Gamma}_{ex,PS}^+(\tilde{S}_p, \tilde{S}_n/\tilde{S}_p)/N$ .

duces the number of scaling variables to two:

$$\tilde{\Gamma}_{ex,PS}^+(\tilde{S}_p, \tilde{S}_n/\tilde{S}_p) = N \int_0^{\tilde{S}_p + \tilde{S}_n} dv \int_0^\infty dw [P_{PS}^+(v, w, \tilde{S}_p, \tilde{S}_n/\tilde{S}_p) - P_{PS,0}^+(v, w, \tilde{S}_p, \tilde{S}_n/\tilde{S}_p)], \quad (50)$$

where  $P_{PS,0}^+ = P_\infty^+(w)$  on the positive stripe and  $P_{PS,0}^+ = -P_\infty^+(w)$  on the negative stripe.  $N$  is the number of periodic cells on the substrate. In analogy to Eq. (49) one has

$$\tilde{\Gamma}_{ex,PS}^+(\tilde{S}_p, \tilde{S}_n/\tilde{S}_p) = N \left\{ \int_0^{\tilde{S}_p + \tilde{S}_n} dv \int_0^\infty dw [P_{PS}^+(v, w, \tilde{S}_p, \tilde{S}_n/\tilde{S}_p)] - (\tilde{S}_p - \tilde{S}_n) \tilde{\Gamma}_\infty^+ \right\}. \quad (51)$$

As compared with the case of a single stripe the periodic arrangement enhances the excess adsorption by the (potentially large) number of lateral repeat units. Figure 12(a) shows that  $\tilde{\Gamma}_{ex,PS}^+ \geq 0$  for  $S_p \geq S_n$ .  $\tilde{\Gamma}_{ex,PS}^+$  vanishes at  $S_n = 0$  because this corresponds to the limiting case of a homogeneous substrate.  $\tilde{\Gamma}_{ex,PS}^+$  also vanishes for  $S_n = S_p$  for symmetry

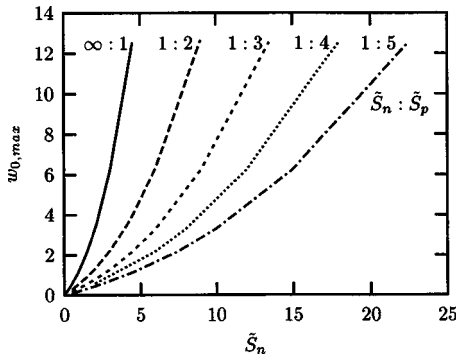


FIG. 13. Dependence of the rescaled length  $w_{0,\max}$  of the tongues within which the order parameter adjacent to a stripe maintains the sign preference of the stripe (compare Fig. 10) on the stripe width  $\tilde{S}_n$  for different ratios  $\tilde{S}_n/\tilde{S}_p$ . The limit  $\tilde{S}_n/\tilde{S}_p \rightarrow \infty$  corresponds to the case of a single stripe of width  $\tilde{S}_p$ . The full curve corresponds to the latter case (see also Fig. 11) and is denoted as  $\infty:1$ .

reasons. The limit  $\tilde{S}_n/\tilde{S}_p \rightarrow \infty$  with  $\tilde{S}_p$  fixed leads to the case of a single stripe of width  $\tilde{S}_p$ ; this corresponds to Fig. 9 up to the factor  $N$ . In Fig. 12(b) the loci of the maxima of the excess adsorption  $\tilde{\Gamma}_{\text{ex,PS}}^+/N$  for different stripe widths  $\tilde{S}_p$  and  $\tilde{S}_n$  are given.

The positive values of the excess adsorption  $\tilde{\Gamma}_{\text{ex,PS}}^+$  are again caused by the tonguelike regions within which the order parameter profile has a definite sign. For  $\tilde{S}_p < \tilde{S}_n$  there is a finite tonguelike region adjacent to each positive stripe within which the order parameter is positive, and it is negative outside of it. For  $\tilde{S}_p \rightarrow \tilde{S}_n$  the tongue length diverges and the tongue boundaries degenerate into two parallel lines orthogonal to the substrate. For  $\tilde{S}_p > \tilde{S}_n$  there are tongues of negative values of the order parameter adjacent to the negative stripes. Figure 13 shows the length  $w_{0,\max}$  of the tongues on the stripe width  $\tilde{S}_n$  for different ratios  $\tilde{S}_n/\tilde{S}_p$ . With increasing ratio  $\tilde{S}_n/\tilde{S}_p \rightarrow \infty$  the limit of a substrate with a single positive stripe of width  $\tilde{S}_p$  in a negative matrix is reached.

#### IV. SUMMARY

Based on mean field theory combined with renormalization group arguments we have studied critical adsorption of fluids at chemically structured substrates. The fluids are either one- or two-component liquids near their gas-liquid critical point or binary liquid mixtures near their critical demixing point. In the first case the order parameter is given by the local total density, in the second case by the local concentration. We have determined the order parameter profiles and suitably defined excess adsorptions for three substrate types: a single chemical step, a single chemical stripe, and a periodic stripe pattern (see Fig. 1). We have obtained the following main results.

(1) The order parameter profiles and the excess adsorption can be described in terms of universal scaling functions [Eqs. (24), (35), (39)–(41), (44), (49), and (51)]. The excess

adsorptions are introduced relative to order parameter profiles at homogeneous substrates (Sec. II and Fig. 2) taken to vary in a steplike way in the lateral direction according to the actual chemical pattern under consideration.

(2) The specific shapes of the scaling functions are determined within mean field theory. For the *chemical step* the full scaling function of the order parameter profiles is shown in Fig. 3 in terms of the scaling variables  $v=x/\xi$  and  $w=z/\xi$  given by the lateral ( $x$ ) and the normal ( $z$ ) coordinates in units of the bulk correlation length  $\xi$ . Lateral cuts through the normalized scaling function with an emphasis on its asymptotic behavior far from the substrate are shown in Fig. 4. For the case of strong adsorption considered here the slopes of the scaling function across the chemical step increase  $\sim w^{-2}$  upon approaching the surface and decay  $\sim e^{-Cw}$  toward the bulk with  $C=1$  above  $T_c$  and  $C<1$  below  $T_c$  (Fig. 5). To a large extent the variation of the full scaling function normal to the surface can be absorbed by rescaling the lateral variation suitably (Fig. 6). The excess adsorption at the chemical step [Eq. (37) and Fig. 7] leads to universal numbers above [Eq. (40)] and below  $T_c$  [Eqs. (39) and (41)].

(3) The lateral variation of the order parameter adjacent to a *single chemical stripe* is shown in Fig. 8 in terms of its suitably normalized scaling function. Figure 8 visualizes the dependence of these structures on the scaled stripe width. Figure 10 illustrates the influence of a chemical stripe of width  $S$  on the adjacent order parameter. The range of this influence, defined as the spatial region of maintaining the preferred sign of the order parameter, generates tonguelike structures which grow with increasing stripe width (Fig. 11). The excess adsorption [Eq. (49)] is described by a universal scaling function in terms of  $\tilde{S}=S/\xi$ , which is minimal for  $\tilde{S} \approx 0.3$  (Fig. 9).

(4) For a *periodic stripe pattern* of  $N$  unit cells the scaling function for the order parameter depends on four scaling variables:  $v$ ,  $w$ ,  $\tilde{S}_p=S_p/\xi$ , and  $\tilde{S}_n=S_n/\xi$  where  $S_p$  and  $S_n$  are the widths of the stripes with positive and negative surface fields, respectively. The range of influence (see point 3 above) of the narrower stripes is again confined to tonguelike structures which grow with increasing stripe width (Fig. 13). The corresponding excess adsorption [Fig. 12(a)] is given by a universal scaling function in terms of  $\tilde{S}_p$  and  $\tilde{S}_n$ , which describes the interpolation between the homogeneous substrate ( $\tilde{S}_n/\tilde{S}_p=0$ ) and a single stripe of width  $\tilde{S}_p$  ( $\tilde{S}_n/\tilde{S}_p=\infty$ ,  $\tilde{S}_p$  fixed). The relation between  $\tilde{S}_p$  and  $\tilde{S}_n$  that yields the maximum excess adsorption is shown in Fig. 12(b).

#### APPENDIX: NUMERICAL METHODS

In the following, we provide some details of the numerical methods we have applied. The order parameter profiles are calculated numerically from Eqs. (13)–(15) by introducing a discrete lattice with finite spatial extensions. The extension of the system perpendicular to the substrate ( $z$  direction) is  $L$ ; the extension in the direction of the inhomogeneity of the substrate ( $x$  direction) is  $B$ . The corresponding lattice spacings are denoted as  $dz$  and  $dx$ . Since the system is

translationally invariant in the  $d-2$  directions perpendicular to the  $x-z$  plane (where  $d$  denotes the spatial dimension of the system), the numerical problem is effectively two dimensional.

For the calculation of the scaling functions these quantities are scaled with the correlation length  $\xi^\pm$  leading to the scaled length  $\tilde{L}$  in the  $w$  direction, the scaled width  $\tilde{B}$  in the  $v$  direction, and the corresponding lattice spacings  $dw$  and  $dv$ , respectively. In order to mimic the characteristics of an infinitely extended system we choose an exponentially decaying continuation of the order parameter profiles as the boundary condition at the distance  $L$  from the substrate. (For the nonantisymmetric profiles we resort to a constant continuation.) In the case of the substrate with a single chemical step or a single stripe we choose the width  $\tilde{B}$  such that the system is sufficiently broad that the influence of the chemical steps at the lateral boundaries is negligible and the order parameter attains the value of the corresponding half-space profile  $P_\infty^\pm(w)$  for infinite surface fields  $\tilde{h}_1 \rightarrow \infty$  or  $P_{h_1}^\pm(w)$  for finite surface fields  $\tilde{h}_1 < \infty$ :  $P_{CS}^\pm(\pm\tilde{B}/2, w) = \pm P_{h_1}^\pm(w)$ ,  $P_{SS}^\pm(\pm\tilde{B}/2, w) = -P_{h_1}^\pm(w)$ . For the substrate with periodic stripes one can focus on a single unit cell so that the scaled width  $\tilde{B}$  is the sum of the stripe widths  $\tilde{S}_p$  and  $\tilde{S}_n$  with periodic boundary conditions:  $P_{PS}^\pm(+\tilde{B}/2, w) = P_{PS}^\pm(-\tilde{B}/2, w)$ . The choices for the width  $\tilde{B}$  and the length  $\tilde{L}$  of the system are not completely independent, i.e., for a given length  $\tilde{L}$  there is

a minimum width  $\tilde{B}$  so that  $\tilde{L}$  and  $\tilde{B}$  span a region in which the order parameter profile is calculated correctly under the chosen boundary conditions. It turns out that a width  $\tilde{B} \geq 16$  is sufficient for the studied range of lengths  $\tilde{L} \leq 20$ . For the substrates with a single stripe the width  $\tilde{B} - \tilde{S}$  of the negative matrix is chosen as  $\tilde{B} - \tilde{S} \geq 16$  and is kept constant for different widths of the stripe. We use the steepest descent method in order to calculate the order parameter profiles. The values of the scaling function  $P(v, w)$  of the order parameter at each lattice point are split into an initial part  $P_{in}(v, w)$  [see the profiles for systems where no healing occurs given by Eqs. (36) and (47)], which is a known solution for a system similar to the one under consideration, and a correction term  $P_{corr}(v, w)$ , which is varied in accordance with the steepest descent method. This procedure is described in detail in Ref. [45]. The excess adsorption depends on the value of the lattice spacings  $dv$  and  $dw$ , respectively, used for its numerical calculation. Therefore we have calculated the excess adsorption for different lattice constants and extrapolated it to  $dv = dw = 0$ . It also depends on the length of the system. Hence we calculated the order parameter profiles for a fixed width  $\tilde{B}$  and different lengths  $\tilde{L}$ . For lengths larger than  $\tilde{L} = 10$  the results are indistinguishable, i.e., for these lengths corrections with respect to an infinitely long system are negligible.

- 
- [1] T. Thorsen, S. J. Maerkl, and S. R. Quake, *Science* **298**, 580 (2002).
- [2] D. Juncker, H. Schmidt, U. Drechsler, H. Wolf, M. Wolf, B. Michel, N. de Rooij, and E. Delamarche, *Anal. Chem.* **74**, 6139 (2002).
- [3] M. Böltau, S. Walheim, J. Mlynek, G. Krausch, and U. Steiner, *Nature (London)* **391**, 877 (1998).
- [4] M. Sprenger, S. Walheim, C. Schäfle, and U. Steiner, *Adv. Mater. (Weinheim, Ger.)* **15**, 703 (2003).
- [5] H. E. Stanley, *Introduction to Phase Transitions and Critical Phenomena* (Clarendon, Oxford, 1971).
- [6] J. Zinn-Justin, *Quantum Field Theory and Critical Phenomena* (Oxford University Press, Oxford, 1989).
- [7] Y. Xia, J. A. Rogers, K. E. Paul, and G. M. Whitesides, *Chem. Rev. (Washington, D.C.)* **99**, 1823 (1999).
- [8] F. S. Bates, *Science* **251**, 898 (1991).
- [9] G. Krausch and R. Magerle, *Adv. Mater. (Weinheim, Ger.)* **14**, 1579 (2002).
- [10] B. Zhao, J. S. Moore, and D. J. Beebe, *Anal. Chem.* **74**, 4259 (2002).
- [11] A. Kumar and G. M. Whitesides, *Appl. Phys. Lett.* **63**, 2002 (1993).
- [12] R. Wang, K. Hashimoto, A. Fujishima, M. Chikuni, E. Kojima, A. Kitamura, M. Shimohigoshi, and T. Watanabe, *Nature (London)* **388**, 431 (1997).
- [13] R. Wang, K. Hashimoto, A. Fujishima, M. Chikuni, E. Kojima, A. Kitamura, M. Shimohigoshi, and T. Watanabe, *Adv. Mater. (Weinheim, Ger.)* **10**, 135 (1998).
- [14] K. Seki and M. Tachiya, *J. Phys. Chem. B* **108**, 4806 (2004).
- [15] S. N. Jasperson and S. E. Schnatterly, *Rev. Sci. Instrum.* **40**, 761 (1969).
- [16] D. Beaglehole, *Physica B* **100**, 163 (1980).
- [17] J.-H. J. Cho and B. Law, *Phys. Rev. E* **65**, 011601 (2001).
- [18] J. Howse, E. Manzanares-Papayanopoulos, I. McLure, J. Bowlers, R. Steitz, and G. H. Findenegg, *J. Chem. Phys.* **116**, 7177 (2002).
- [19] J. Penfold and R. K. Thomas, *J. Phys.: Condens. Matter* **2**, 1369 (1990).
- [20] P. N. Thirtle, Z. X. Li, R. K. Thomas, A. R. Rennie, S. K. Satija, and L. P. Sung, *Langmuir* **13**, 5451 (1997).
- [21] S. Dietrich and R. Schack, *Phys. Rev. Lett.* **58**, 140 (1987).
- [22] M. Geoghegan and G. Jannink, *Proc. R. Soc. London, Ser. A* **454**, 659 (1998).
- [23] H. Gröll and D. Woermann, *J. Chem. Phys.* **105**, 2527 (1996).
- [24] G. Rother, D. Woywod, M. Schoen, and G. H. Findenegg, *J. Chem. Phys.* **120**, 11864 (2004).
- [25] G. Flöter and S. Dietrich, *Z. Phys. B: Condens. Matter* **97**, 213 (1995).
- [26] B. M. Law, *Prog. Surf. Sci.* **66**, 159 (2001).
- [27] J. Drelich, J. D. Miller, A. Kumar, and G. M. Whitesides, *Colloids Surf., A* **93**, 1 (1994).
- [28] H. Gau, S. Herminghaus, P. Lenz, and R. Lipowsky, *Science* **283**, 46 (1999).
- [29] M. Geoghegan and G. Krausch, *Prog. Polym. Sci.* **28**, 261

- (2003).
- [30] K. Binder, in *Phase Transitions and Critical Phenomena*, edited by C. Domb and J. L. Lebowitz (Academic, London, 1983), Vol. 8, p. 1.
- [31] H. W. Diehl, in *Phase Transitions and Critical Phenomena*, edited by C. Domb and J. L. Lebowitz (Academic, London, 1986), Vol. 10, p. 75.
- [32] M. E. Fisher and P.-G. de Gennes, *C. R. Seances Acad. Sci., Ser. B* **287**, 207 (1978).
- [33] D. S. Smith, B. M. Law, M. Smock, and D. P. Landau, *Phys. Rev. E* **55**, 620 (1997).
- [34] G. Palagyi and S. Dietrich, *Phys. Rev. E* **70**, 046114 (2004).
- [35] C. Bauer, S. Dietrich, and A. O. Parry, *Europhys. Lett.* **47**, 474 (1999).
- [36] C. Bauer and S. Dietrich, *Phys. Rev. E* **60**, 6919 (1999).
- [37] M. Brinkmann and R. Lipowsky, *J. Appl. Phys.* **92**, 4296 (2002).
- [38] M. Schneemilch, N. Quirke, and J. R. Henderson, *J. Chem. Phys.* **118**, 816 (2003).
- [39] H. Ez-Zahraouy, L. Bahmad, and A. Benyoussef, e-print, cond-mat/0404199.
- [40] A. J. Bray and M. A. Moore, *J. Phys. A* **10**, 1927 (1977).
- [41] T. W. Burkhardt and H. W. Diehl, *Phys. Rev. B* **50**, 3894 (1994).
- [42] J. C. Le Guillou and J. Zinn-Justin, *J. Phys. (Paris), Lett.* **46**, L137 (1985).
- [43] E. Brézin and J. Zinn-Justin, *Phys. Rev. B* **14**, 3110 (1976).
- [44] This terminology refers to the case of a simple fluid below the critical temperature where within mean field theory the corresponding scaling function for the interface between the liquid phase and the vapor phase is given by Eq. (25).
- [45] F. Schlesener, A. Hanke, and S. Dietrich, *J. Stat. Phys.* **110**, 981 (2003).